Generation of ultra-flat optical frequency comb using a balanced driven dual parallel Mach–Zehnder modulator

Jian Wang (王 建)[1,2], Haiwen Cai (蔡海文)[1,*], Dijun Chen (陈迪俊)[1], and Ronghui Qu (瞿荣辉)[1]

[1]*Shanghai Key Laboratory of All Solid-State Laser and Applied Techniques, Shanghai Institute of Optics and Fine Mechanics, Chinese Academy of Sciences, Shanghai 201800, China*

[2]*University of Chinese Academy of Sciences, Beijing 100049, China*

**Corresponding author: hwcai@siom.ac.cn*

Received January 6, 2015; accepted April 23, 2015; posted online May 26, 2015

We propose and experimentally demonstrate an ultra-flat optical frequency comb (OFC) generator by a balanced driven dual parallel Mach–Zehnder modulator. Five- and seven-tone OFC with exactly equal intensity can be generated theoretically. Experimentally obtained five- and seven-tone OFC with flatness of 0.6 and 1.26 dB are demonstrated, respectively, which agrees well with the theoretical results.

OCIS codes: 060.1660, 060.2330, 060.2380.

doi: 10.3788/COL201513.060604.

The optical frequency comb (OFC) generation with equal frequency spacing, equal spectrum power, and flexible tunability is highly desired in many fields. OFC generators offer attractive and promising applications such as for generating precisely spaced optical wavelengths for dense wavelength-division multiplexing[1], frequency metrology[2], optical clock[3], and so on. Generally speaking, mode-locked lasers (MLLs) and electro-optic modulator (EOM)-based OFC generators are potential candidates. MLL-based generators suffer from poor tunability and stability since the resonator is easily influenced by environment.

OFC generation for flat combs via electro-optic modulation is a potential and economic method, since multiple channels can be generated with few lasers and could be scalable. In most cases, it is important to generate frequency combs with good spectral flatness. However, it is difficult to generate OFC with good flatness, because the intensity of each mode is governed by Bessel function. Schemes such as cascaded amplitude/phase modulators, and an amplitude modulator cascaded with a phase modulator provide an OFC with dozens of lines have been proposed[4–9] which need multiple channel radio frequency (RF) signals with different powers, and different frequencies to drive the multiple EOMs, resulting in a costly and complex structure with poor tenability. Also, OFC generation scheme based on single sideband modulation recirculating frequency shifter has also been proposed adopting by dual parallel Mach–Zehnder modulator (DPMZM) inserted in a recirculating loop[10]. In addition, single EOM such as dual driven Mach–Zehnder modulator (DDMZM), DPMZM-based OFC generator is recently demonstrated. OFC generator with multi-lines can be obtained by the unbalanced and nonlinear (super-amplified) driven of the DDMZM theoretically[11]. Single-phase-modulator-based flat OFC generator is also demonstrated with flatness of 0.8 dB among nine comb lines[12]. The only ultra-flat OFC generator with equal spectral intensity is by unbalanced driven two parallel arms of the DPMZM[13]. Five- and seven-tone OFC with equal spectral intensity is obtained theoretically and experimentally, and five- and seven-tone combs with 0 dB flatness is generated theoretically. Experiments agree well with the theoretical results for less than 0.1 dB for five-tone combs and less than 1 dB for seven-tone combs. In the process of ultra-flat OFC generation in Ref. [13], frequency chirp is present and its value is changeable. For unbalanced driven DPMZM, frequency chirp is often generated, and positive frequency chirp will degrade the performance of system on account of fiber dispersion in long-haul optical fiber communication system[14].

In this Letter, we propose and experimentally demonstrate another flexible ultra-flat OFC generator with a balanced driven DPMZM by outputs of a broadband 90° hybrid coupler. Free chirp is obtained in the generation of ultra-flat OFC with our configuration. According to the DPMZM modulation model, both a five- and seven-tone OFC with 0 dB flatness are theoretically generated. Applying the theoretical analysis as a guideline, a five-tone and seven-tone OFC with flatness within 0.6 and 1.26 dB is experimentally achieved, which is in agreement with the theoretical results.

As shown in Fig. 1, the DPMZM is an integrated optical device composed of a parent Mach–Zehnder interferometer which is embedded by two child MZIs (MZI1 and MZI2). MZI1 and MZI2 are balanced-driven by RF signals with 90° phase difference. Assuming the angular frequency and amplitude of the sinusoidal RF signal are ω and V, respectively. The electric field at the output (E_{out}) of the DPMZM can be expressed as

$$E_{\rm out}=\frac{E_{\rm in}}{4}\left\{\exp\left(j\frac{\pi}{V_\pi}V_{\rm bias1}\right)\exp\left[j\frac{\pi}{2V_\pi}V\sin(\omega t)\right]\right.$$
$$+\exp\left[-j\frac{\pi}{2V_\pi}V\sin(\omega t)\right]+\exp\left[j\frac{\pi}{V_\pi}V_{\rm bias3}\right]$$
$$\times\left\{\exp\left(j\frac{\pi}{V_\pi}V_{\rm bias2}\right)\exp\left[j\frac{\pi}{2V_\pi}V\sin(\omega t+\varphi)\right]\right.$$
$$\left.\left.+\exp\left[-j\frac{\pi}{2V_\pi}V\sin(\omega t+\varphi)\right]\right\}\right\} \quad (1)$$

where $E_{\rm in}$ represents the electric field of the incident continuous wave (CW) laser; $V_{\rm bias1}$, $V_{\rm bias2}$, and $V_{\rm bias3}$ represent the three bias voltages. V_π represents the half-wave voltage. Equation (1) can be expanded using Bessel function expansion

$$E_{\rm out}=\frac{E_{\rm in}}{4}\left\{\sum_{n=-\infty}^{\infty}[\exp(jV_{\rm a})+(-1)^n]J_{\rm n}(\beta)\exp(jn\omega t)+\exp(jV_c)\left\{\sum_{n=-\infty}^{\infty}[\exp(jV_b)+(-1)^n]J_{\rm n}(\beta)\exp[jn(\omega t+\varphi)]\right\}\right\}, \quad (2)$$

where $V_a=\pi V_{\rm bias1}/V_\pi$, $V_b=\pi V_{\rm bias2}/V_\pi$, $V_c=\pi V_{\rm bias3}/V_\pi$, and $\beta=\pi V/(2V_\pi)$.

Intensities of the n-order sidebands are then expressed as

$$\begin{cases} I_{n=2k}=\cos^2\left(\frac{1}{2}V_a\right)J_n^2(\beta)+\cos^2\left(\frac{1}{2}V_b\right)J_n^2(\beta)+2\cos\left(\frac{1}{2}V_a\right) \\ \quad *\cos\left(\frac{1}{2}V_b\right)J_n^2(\beta)\cos\left(\frac{1}{2}V_a-\frac{1}{2}V_b-V_c+n\varphi\right) \\ I_{n=2k-1}=\sin^2\left(\frac{1}{2}V_a\right)J_n^2(\beta)+\sin^2\left(\frac{1}{2}V_b\right)J_n^2(\beta)+2\sin\left(\frac{1}{2}V_a\right) \\ \quad *\sin\left(\frac{1}{2}V_b\right)J_n^2(\beta)\cos\left(\frac{1}{2}V_a-\frac{1}{2}V_b-V_c+n\varphi\right)\varphi=\pi/2. \end{cases} \quad (3)$$

Solving the equation $I_{2k-1}=I_{-(2k-1)}$, we can get

$$\frac{1}{2}V_a-\frac{1}{2}V_b-V_c=l\pi, \qquad (l=0,1,\ldots) \quad (4)$$

The frequency chirp factor is[15,16]

$$\alpha=\frac{I*(d\phi/dt)}{dI/dt} \quad (5)$$

where

$$I*(d\phi/dt)=\sin\left[\frac{\pi}{2V_\pi}V_{\rm bias1}-\frac{\pi}{2V_\pi}V_{\rm bias2}-\frac{\pi}{V_\pi}V_{\rm bias3}\right]\left\{\cos\left[\frac{\pi}{2V_\pi}(V_1(t)+V_{\rm bias1})\right]\right.$$
$$\left.*\sin\left[\frac{\pi}{2V_\pi}(V_2(t)+V_{\rm bias2})\right]V_2'(t)-\sin\left[\frac{\pi}{2V_\pi}(V_1(t)+V_{\rm bias1})\right]\cos\left[\frac{\pi}{2V_\pi}(V_2(t)+V_{\rm bias2})\right]V_1'(t)\right\},$$
$$dI/dt=\sin\left[\frac{\pi}{V_\pi}(V_1(t)+V_{\rm bias1})\right]V_1'(t)+\sin\left[\frac{\pi}{V_\pi}(V_2(t)+V_{\rm bias2})\right]V_2'(t)$$
$$+\sin\left[\frac{\pi}{2V_\pi}V_{\rm bias1}-\frac{\pi}{2V_\pi}V_{\rm bias2}-\frac{\pi}{V_\pi}V_{\rm bias3}\right]\left\{\cos\left[\frac{\pi}{2V_\pi}(V_1(t)+V_{\rm bias1})\right]\sin\left[\frac{\pi}{2V_\pi}(V_2(t)+V_{\rm bias2})\right]V_2'(t)\right.$$
$$\left.+\sin\left[\frac{\pi}{2V_\pi}(V_1(t)+V_{\rm bias1})\right]\cos\left[\frac{\pi}{2V_\pi}(V_2(t)+V_{\rm bias2})\right]V_1'(t)\right\}.$$

The expression of the chirp parameter contains a factor of $\sin[\frac{\pi}{2V_\pi}V_{\rm bias1}-\frac{\pi}{2V_\pi}V_{\rm bias2}-\frac{\pi}{V_\pi}V_{\rm bias3}]$ in the numerator of the fraction which cannot be eliminated.

From Eq. (4), we know that the chirp of the DPMZM with our configuration $\alpha=0$.

The equation $I_0=I_1$ can be expressed as

$$\sin^2\left(\frac{1}{2}V_a\right)J_1^2(\beta)+\sin^2\left(\frac{1}{2}V_b\right)J_1^2(\beta)$$
$$=\cos^2\left(\frac{1}{2}V_a\right)J_0^2(\beta)+\cos^2\left(\frac{1}{2}V_b\right)J_0^2(\beta)$$
$$+2\cos\left(\frac{1}{2}V_a\right)\cos\left(\frac{1}{2}V_b\right)J_0^2(\beta). \quad (6)$$

The equation $I_0=I_2$ can be expressed as

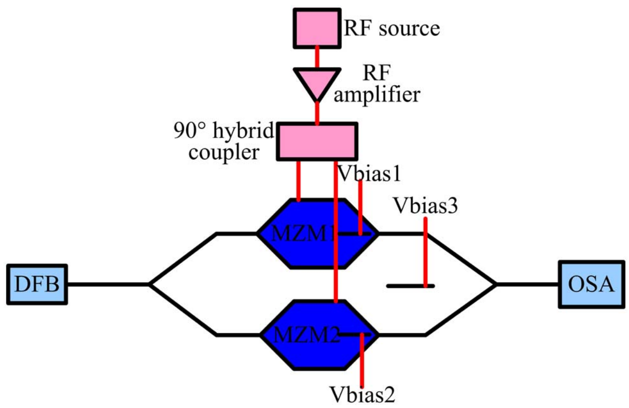

Fig. 1. Schematic diagram of the proposed ultra-flat OFC generator.

$$\cos^2\left(\frac{1}{2}V_a\right)J_0^2(\beta)+\cos^2\left(\frac{1}{2}V_b\right)J_0^2(\beta)$$
$$+2\cos\left(\frac{1}{2}V_a\right)\cos\left(\frac{1}{2}V_b\right)J_0^2(\beta)\cos\left(\frac{1}{2}V_a-\frac{1}{2}V_b-V_c\right)$$
$$=\cos^2\left(\frac{1}{2}V_a\right)J_2^2(\beta)+\cos^2\left(\frac{1}{2}V_b\right)J_2^2(\beta)$$
$$+2\cos\left(\frac{1}{2}V_a\right)\cos\left(\frac{1}{2}V_b\right)J_2^2(\beta)$$
$$\times\cos\left(\frac{1}{2}V_a-\frac{1}{2}V_b-V_c+\pi\right). \quad (7)$$

Equations (6) and (7) can be simplified as

$$\frac{\left[\cos\left(\frac{1}{2}V_a\right)+\cos\left(\frac{1}{2}V_b\right)\right]^2}{\left(1+2\cos\left(\frac{1}{2}V_a\right)\cos\left(\frac{1}{2}V_b\right)\right)}=\frac{2J_1^2(\beta)}{(J_0^2(\beta)+J_1^2(\beta))}, \quad (8)$$

$$\frac{2\cos\left(\frac{1}{2}V_a\right)\cos\left(\frac{1}{2}V_b\right)}{\cos^2\left(\frac{1}{2}V_a\right)+\cos^2\left(\frac{1}{2}V_b\right)}=\frac{(J_0^2(\beta)-J_2^2(\beta))}{(J_0^2(\beta)+J_2^2(\beta))}. \quad (9)$$

There is 1 degree of freedom in Eqs. (8) and (9). For one β, there may be one pair of corresponding values of (V_a, V_b). Equations (4), (8), and (9) can be easily satisfied by groups of β, (V_a, V_b).

Solving Eqs. (8) and (9), and setting $m=\frac{2J_1^2(\beta)}{J_0^2(\beta)+J_1^2(\beta)}$, $n=\frac{J_0^2(\beta)-J_2^2(\beta)}{J_0^2(\beta)+J_2^2(\beta)}$, we can get

$$\begin{cases}\cos^2\left(\frac{1}{2}V_a\right)+\cos^2\left(\frac{1}{2}V_b\right)=\frac{2m}{2+n-2mn}=k_1\\ \cos\left(\frac{1}{2}V_a\right)*\cos\left(\frac{1}{2}V_a\right)=\frac{mn}{2+n-2mn}=k_2.\end{cases} \quad (10)$$

Then $\cos(V_a/2)$ and $\cos(V_b/2)$ can be derived as follows

$$\begin{cases}\cos\left(\frac{1}{2}V_a\right)=\frac{\pm\sqrt{k_1+2k_2}\pm\sqrt{k_1-2k_2}}{2}\\ \cos\left(\frac{1}{2}V_b\right)=\frac{\pm\sqrt{k_1+2k_2}\mp\sqrt{k_1-2k_2}}{2}.\end{cases} \quad (11)$$

From Eq. (11), V_a and V_b can be obtained, and then from Eqs. (4), we can get V_c.

There is 1 degree of freedom for Eqs. (8) and (9). For a given β, V_a and V_b that satisfy Eq. (11) can meet requirement of $I_0=I_{\pm1}=I_{\pm2}$. The curves in Fig. 2 are values of V_a and V_b for different values of β. The values of $V_a=0$ or $V_b=0$ mean that the corresponding amplitude of RF signal have no five-tone OFC with equal intensity no matter how you adjust V_a and V_b.

Furthermore, an OFC with more equal tones can be generated with the DPMZM. For $I_{\pm1}=I_{\pm3}$, we can get

$$J_1^2(\beta)=J_3^2(\beta). \quad (12)$$

Equations (8), (9), and (12) are then satisfied, resulting in the seven-tone OFC with exactly equal spectral intensity. In addition, it is manifested that seven-tone combs is the largest number of equal spectral intensity tones that we can obtain using the DPMZM with this configuration theoretically.

Based on the theoretical analysis, a corresponding experiment was performed using a commercially available DPMZM LN86 with half-wave voltage ~4.1 V. As shown in Fig. 1, a 7 dBm CW laser (FRL15DCWD) with wavelength of 1550 nm is launched into the DPMZM. Frequency of 4.8 GHz RF signal from RF source is amplified by gain variable RF amplifier (JDS Uniphase H301) and then injected into a 90° hybrid coupler (Pulsar QS-8). The dual RF ports of the DPMZM are balanced driven by RF outputs of the coupler. For a proper β, by adjusting V_{bias1}, V_{bias2}, and V_{bias3}, an OFC with five tones is generated. The output of the DPMZM is measured with an optical spectrum analyzer (OSA).

For example, for $\beta=0.9$, the theoretically calculated values for amplitude of the RF signals and the bias voltages are $V=0.57V_\pi$, $V_a=2.15$, $V_b=2.37$, and $V_c=6.17$, i.e., $V_{\text{bias1}}=0.68V_\pi$, $V_{\text{bias2}}=0.75V_\pi$, and $V_{\text{bias3}}=1.96V_\pi$, which satisfy the requirements of flat five-tone OFC, as shown in Fig. 3(a). The intensity of

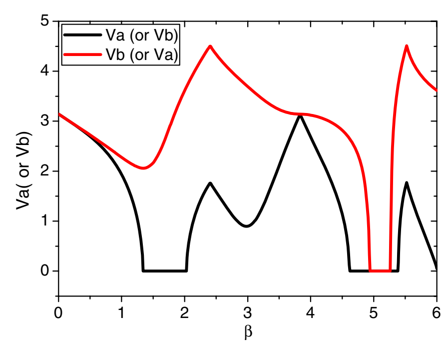

Fig. 2. Values of V_a and V_b for different β.

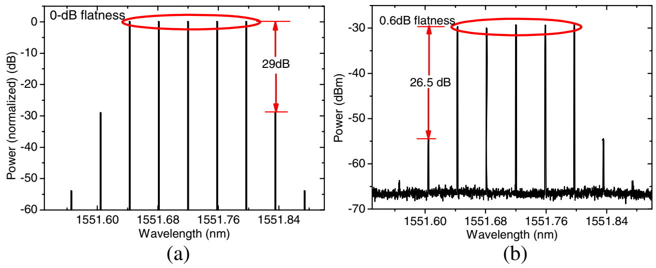

Fig. 3. Spectral of the generated five-tone OFC with the proposed configuration: (a) theoretical; (b) experimental.

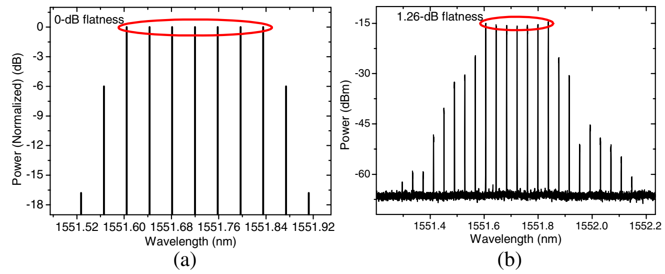

Fig. 4. Spectral of the generated seven-tone OFC with the proposed configuration: (a) theoretical; (b) experimental.

the third-order sideband is 29 dB lower than that of the flat five-tone combs.

While five-tone OFC is achieved experimentally for $V = 0.57V_\pi$ of the RF signals, the sets of the bias voltages of the three MZIs are as follows: $V_{\text{bias1}} = 2.8$ V, $V_{\text{bais2}} = 3.1$ V, and $V_{\text{bias3}} = 8.2$ V, i.e., $V_{\text{bias1}} = 0.7V_\pi$, $V_{\text{bias2}} = 0.76V_\pi$, and $V_{\text{bias3}} = 2V_\pi$, this is, corresponding to $V_a = 2.20$, $V_b = 2.37$, and $V_c = 6.28$. From the aforementioned values, we can see that the experimental values are well consistent with the theoretical ones. Figure 3(b) shows the experimentally generated spectrum. As can be seen in Fig. 3(b), the flatness is measured to be 0.6 dB and the intensity of the third-order sideband is 26.5 dB lower than that of the flat five-tone combs. The resolution of the OSA APEX 2041B in our work is set at 5 MHz. As seen in Fig. 3, the experimental results agree with the theoretical analysis.

Equation (11) requires $\beta = 3.05$ or 5.14, while for $\beta = 5.14$, the value for V_a (or V_b) does not exist. So $\beta = 3.05$, $V_a = \pm 0.93$, $V_b = \pm 3.64$ (or $V_a = \pm 3.64$, $V_b = \pm 0.93$), that is, $V = (\beta/\pi) * 2V_\pi = 1.94V_\pi$, $V_{\text{bias1}} = \pm 0.3V_\pi$, and $V_{\text{bias2}} = \pm 1.16V_\pi$ is the value that suffices seven-tone OFC with equal spectral intensity with our experimental configuration. Figure 4(a) shows the spectrum of the theoretically generated seven-tone OFC with 0 dB flatness.

Seven-tone OFC generation was obtained experimentally in our configuration in Fig. 4. For $V = 1.94V_\pi$ RF signal, when preferable flat seven-tone OFC combs are achieved, the bias voltages are set as follows: $V_{\text{bias1}} = -1.2$ V, $V_{\text{bias2}} = -4.9$ V, and $V_{\text{bias3}} = -2.0$ V, i.e., $V_{\text{bias1}} = -0.3V_\pi$, $V_{\text{bias2}} = -1.17V_\pi$, and $V_{\text{bias3}} = 0.51V_\pi$, this is, corresponding to $V_a = -0.94$, $V_b = -3.67$, and $V_c = 1.57$, while the theoretically calculated values for the three biases are $V_a = -0.93$, $V_b = -3.64$, and $V_c = 1.36$ as depicted previously. Figure 4(b) presents the spectrum of the experimentally generated seven-tone OFC, as shown in Fig. 4(b), the flatness of the generated seven-tone OFC is measured to be within 1.26 dB. For the flat five- and seven-tone OFC generation, the error between theoretical results and experimental results is caused by loss of voltage because of impendence of electrical bias port.

The power difference of the broadband 90° hybrid coupler can generate small unflatness among the powers of generated comb lines, and so is the phase difference of the coupler. The maximum amplitude imbalance of the two outputs of the broadband 90° hybrid coupler in our work for 0.5–10 GHz RF signals is 1.6 dB, and maximum phase error of the two outputs is 8°. In the work, we varied the frequency of the RF source from 0.5 to 10 GHz; the flatness of the generated five-tone and seven-tone OFCs maximally reach 1.1 and 2.3 dB, respectively.

In conclusion, we propose a simple and reliable means of OFC generator with exactly equal spectral intensity using a balanced driven DPMZM with free chirp. Fine-tone OFC with flatness within 0.6 dB is experimentally obtained using the DPMZM dispense of wave-shaping filter. Moreover, a seven-tone OFC with flatness within 1.26 dB is experimentally achieved. In addition, frequency spacing of the generated ultra-flat OFC is tunable within the bandwidth of the employed DPMZM and 90° hybrid coupler.

References

1. M. Fujiwara, M. Teshima, J. I. Kani, H. Suzuki, N. Takachio, and K. Iwatsuki, J. Lightwave Technol. **21**, 2705 (2003).
2. M. Xue, S. Pan, C. He, R. Guo, and Y. Zhao, Opt. Lett. **38**, 4900 (2013).
3. S. B. Papp, K. Beha, P. Del'Haye, F. Quinlan, H. Lee, K. J. Vahala, and S. A. Diddams, Optica **1**, 10 (2014).
4. T. Yamamoto, T. Komukai, K. Suzuki, and A. Takada, J. Lightwave Technol. **27**, 4297 (2009).
5. R. Wu, V. R. Supradeepa, C. M. Long, D. E. Leaird, and A. M. Weiner, Opt. Lett. **35**, 3234 (2010).
6. J. Zhang, N. Chi, J. Yu, Y. Shao, J. Zhu, B. Huang, and L. Tao, Opt. Express **19**, 12891 (2011).
7. Y. Dou, H. Zhang, Y. Wang, and M. Yao, Chin. Opt. Lett. **11**, 070603 (2013).
8. C. Zhang, D. Sun, W. Xie, Z. Xia, S. Wang, H. Shi, Y. Tong, Y. Dong, and W. Hu, Chin. Opt. Lett. **12**, 020602 (2014).
9. J. Li, J. Lin, X. Zhang, L. Xi, X. Tang, and Y. Qiao, Chin. Opt. Lett. **13**, 010605 (2015).
10. Y. Yu, C. Lei, M. Chen, H. Chen, S. Yang, and S. Xie, Chin. Opt. Lett. **12**, 100601 (2014).
11. T. Sakamoto, T. Kawanishi, and M. Izutsu, Opt. Lett. **32**, 1515 (2007).
12. S. Ozharar, F. Quinlan, I. Ozdur, S. Gee, and P. J. Delfyett, IEEE Photon. Technol. Lett. **20**, 36 (2008).
13. Q. Wang, L. Huo, Y. Xing, and B. Zhou, Opt. Lett. **39**, 3050 (2014).
14. S. K. Kim, O. Mizuhara, Y. K. Park, L. D. Tzeng, Y. S. Kim, and J. Jeong, J. Lightwave Technol. **17**, 1320 (1999).
15. H. Kim and A. H. Gnauck, IEEE Photon. Technol. Lett. **14**, 298 (2002).
16. F. Koyama and K. Iga, J. Lightwave Technol. **6**, 87 (1988).